

ZnS NANOPARTICLES SYNTHESIZED THROUGH CHEMICAL AGGREGATION USING POLYETHYLENEIMINE THAT WORKS AS BOTH A STABILIZER AND A COMPLEXING AGENT

A. G. ROJAS-HERNÁNDEZ^a, K. J. MENDOZA-PEÑA^b, E. TROYO-VEGA^a,
C. G. PÉREZ-HERNÁNDEZ^b, S. MUNGUÍA-RODRÍGUEZ^b, T. MENDIVIL-
REYNOSO^{a,b}, L. P. RAMÍREZ-RODRÍGUEZ^b, R. OCHOA-LANDÍN^b,
M. E. ALVAREZ-RAMOS^b, A. DE LEON^{c*}, S. J. CASTILLO^a

^a*Departamento de Investigación en Física, Universidad de Sonora, Hermosillo, Sonora, México. CP 83000*

^b*Departamento de Física, Universidad de Sonora, Hermosillo, Sonora, México. CP 83000²*

^c*Departamento de Ciencias Químico-Biológicas, Universidad de Sonora, Hermosillo, Sonora, México. CP 83000*

The main purpose of this study is to present a simplified and short process for the growth of zinc sulfide (ZnS) nanoparticles from five strategic precursors: zinc acetate, polyethyleneimine, thioacetamide, thiourea and rongalite. The first characterization is UV-vis spectrum, the next is the Tauc model to calculate the direct energy bandgap which was 3.84 eV, subsequently TEM micrographs are presented. With this technique, hexagonal crystallographic planes can be observed, fitting the PDF#83-2377 pattern. Furthermore, some particles with diameters between 25 and 29 nm which support the nanostructured nature of the compound, were found. In addition, zinc sulfide nanoparticles in suspension upon glass plane substrates were deposited through drop coating in order to observe nanoparticle agglomerations with the AFM technique. Finally, Raman dispersion and FTIR were measured and correlated.

(Received November 9, 2016;; Accepted January 17, 2017)

Keywords: ZnS nanoparticles, polyethyleneimine, complexing agent, stabilizer

1. Introduction

In recent years, nanoparticles have been extensively studied due to their potential uses in several areas including energy conversion, electronics, medicine, catalysis and optoelectronics.¹ Many unique properties of nanomaterials are strongly related to their size and shape. At the present time there are several studies to get desired morphologies with decreased defects. Most studies of ZnS NPs are of superficial disorders and quantum confinement of electrons. The quantum confinement of excitons in nanostructured semiconductors widens the bandgap. Thus, ZnS nanoparticles are a strong candidate for optoelectronic applications. The high conductivity in ZnS nanoparticles is explained by a wide disorder on the surface of nanoparticles². Bulk ZnS has a direct bandgap of 3.7 eV^{3,4} and the bandgap can be tuned mainly in the UV region. The bandgap increases while size decreases from bulk to nanoscale^{5,6}. ZnS absorbs humidity and is oxidized in air. This makes it less stable like a pure compound in nature. On the synthesis of nanoparticles it is necessary to use surfactants in order to cover the nanoparticles with a specific agent to avoid cluster formation or superficial reactions.⁷

ZnS materials are important for a variety of applications. For instance, photoconduction, solar cells, field effect transistors, sensors, transducers, optical covers, light emission, biological labels, electroluminescent devices, displays, quantum dot lasers and fungicides. Several methods are available to synthesize ZnS nanoparticles. For example, pulsed laser ablation, electrochemical fabrication, the solvothermal and sol-gel methods, chemical vapor deposition, among others.⁸

* Corresponding author: d_aned@hotmail.com

2. Experimental Results and Discussion

The experimental details for the zinc sulfide nanoparticles synthesis are the following: for the reaction, analytical grade reagent solutions were prepared: A) tetra hydrated zinc acetate (0.4M), B) polyethylenimine: water (3.5:50 vol.), C) thioacetamide (0.1M), D) thiourea (1 M) and E) Rongalite (1M). To prepare the zinc sulfide nanoparticles (ZnS NP's) the formulation consists of adding 0.25 mL of solution A to 0.5 mL of solution B. Then ultrasonic vibrations are applied for 2 minutes. After that, 0.05 mL of solution C are added. Next, the mixture is exposed to ultrasonic vibrations again for 2 minutes. Afterwards, 0.1 mL of solution D and 0.1 ml of solution E undergo the same level of ultrasonic vibrations and are then heated at 90°C during 10 minutes. The obtained nanoparticles are in suspension, with a slightly yellowish color probably due to the preparation media. After several weeks went by, it turned mildly misty. The optical characterization equipment used was a Cary 60 UV-Vis to obtain the absorption response spectrum and from here the direct band gap value was obtained. For the TEM micrographs we used a JEOL JEM – 2010F, the Raman dispersion measurement was carried out by using a micro Raman X'plora BXT40 with a resolution of 2400T, and the FTIR spectrum was measured by Nicolette, protégé-460.

The UV-vis results will be described below. Fig. 1 depicts the absorption optical response for the suspension of ZnS nanoparticles. As we can observe there is a shouldered absorption edge whose shape could be due to compounds that remain in suspension that lead to an estimate of the energy bandgap of ZnS NPs through our procedure. Figure 2 shows the bandgap calculation from the Tauc process. The obtained value was of 3.84 eV which can be compared to the reported bulk value of 3.7 eV. This is a first indicator of nanocrystals which induces a quantum confinement. On the other hand, we performed HRTEM micrographs in order to investigate the structure of the ZnS obtained. In a copper grid hold sample a drop of the suspension containing the ZnS particles was deposited. It was then dried under the action of a mechanical vacuum pump and afterwards it was introduced into the TEM microscope chamber. Figure 3 consists of two images, the inset depicts the micrograph with an indicated magnification scale of 200 nm, whereas the main image shows several ZnS particles where some of them were measured diametrically, and their measurements were between 25 and 29 nm.

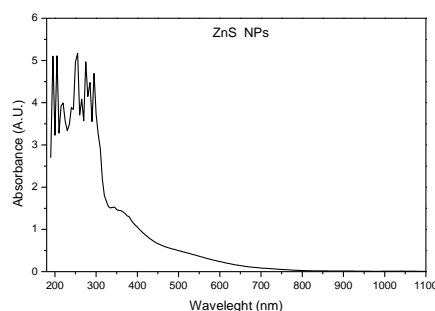


Fig. 1. Absorbance curve of the ZnS Nanoparticles in the UV –vis range

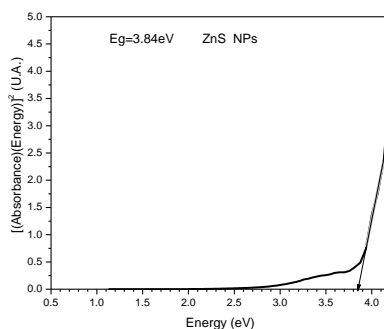


Fig. 2. Bandgap direct compute of the ZnS Nanoparticles synthesized.

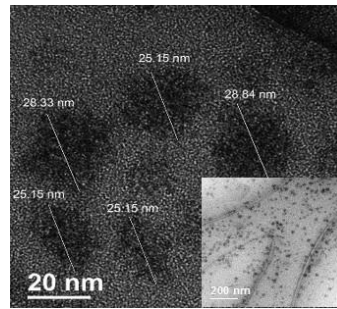


Fig. 3. HRTEM micrographs in the upper case with the same region but with two different scales

Fig. 4 was also built from HRTEM characterization, where the main or large image is a contrast image of the transmitted electron beam through the sample of the ZnS particles. As it can be observed, four interplanar distances of 2.93, 3.11, 3.21 and 3.31 nm are shown. The right inset justifies the measurement of 3.11 nm, where the upper inset displays the reduced Fourier transform of the contrast image and the application of a mismatched mask. Based on the crystallographic database, we found that the series of interplanar distances are characteristic of a reported hexagonal structures for the ZnS with the PDF#83-2377 pattern.

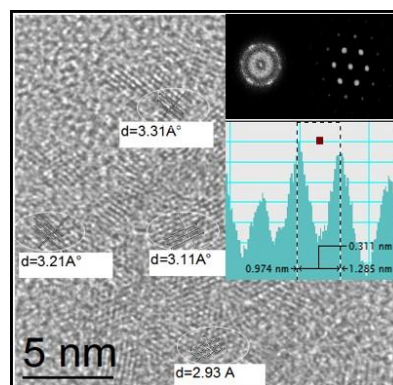


Fig. 4. Some interplanar distances measured in a ZnS NPs micrograph with an indicated 5 nm scale; a profile image and; its Fourier Transform are shown

By drop coating a sample upon a glass slide surface was dispersed and prepared. After it was dry, the two AFM images presented in Fig. 5 were obtained. The two typical views, top and perspective, left and right images, respectively are shown. Some material agglomerates of the ZnS NPs can be observed. Their heights are between 30 and 47 nm, and their base diameters range from 100 to 500 nm.

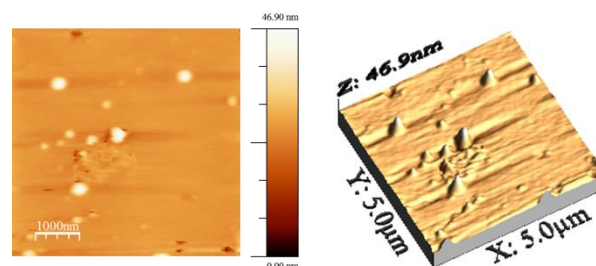


Fig. 5. AFM results, in the left image one 2D morphological image is shown, and in the right case 3D morphological behavior

Other characterizations practiced on this system of ZnS NPs are presented on the same frame, see Figure 6. These characterizations are two plots corresponding to Raman dispersions using red and blue Lasers to stimulate the dispersion; and the FTIR Transmission spectrum. The main reason to mix these three curves is to correlate their band peaks and to interpret the kind of transitions that can be carried out inside this material system. Nine of the resulting signals have been identified or correlated among them, as it is shown in Table 1.

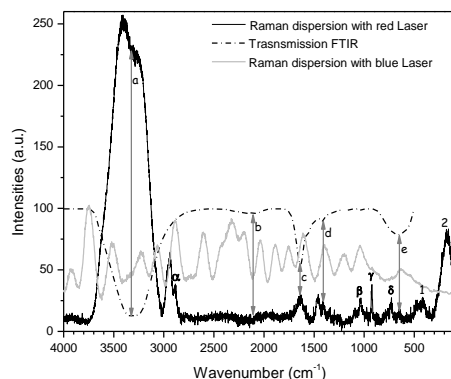


Fig. 6. Raman and FTIR CdS nanoparticle results

The Latin labeled signals (a, b, c, d and e) that are shown in figure 6, reveal a certain coincidence among the absorptions of the FTIR spectrum with signals on the Raman spectrum done by using a red laser. On the other hand, the Greek labeled signals (α , β , γ , δ , 1 and 2) that are shown in Figure 6, reveal coincidences among Raman spectra for both red and blue lasers.

Table 1. Compared values of measured wavenumbers versus some reported ones in the literature and their associated vibration modes

Label	Wavenumber (cm-1)	Mismatching	Vibration modes	Reference
a	3326	3000-3500	$\nu(\text{OH})$	9
b	2115	2370	$s(\text{C-O})$	10
c	1639	1638	H_2O	9
d	1412	1398	$[\text{S}]_{\text{vs}}[\text{COO}^-]$	11
e	650	645	$[\text{TO}+\text{LO}]_{\text{H,M,L}}$	12
α	2885	2882	C-H	13
β	1033	1010	ZnS	10
γ	923	915	C-C	14
δ	728	728	$\text{CO}_3^{2-} \nu_2$	15
ϵ	410	414	$[\text{LO}+\text{TA}]_{\text{L,M}}$	12
1	223	224	$[\text{2LA}]_{\text{M-K}}$	12
2	179	181.3	$[\text{2TA}]_{\text{X}}$	13

S symmetric stretching peak frequency

TO Transversal Optic vibration, *TA* Transversal Acoustic vibration

LO longitudinal Optic vibration, *LA* longitudinal Acoustic vibration.

All exhibit a broad absorption band in the 3000-3500 cm^{-1} region that is associated with $\nu(\text{OH})$ stretching vibrations of liquid water with disordered hydrogen bonds. The band at 2370 cm^{-1} is due to the C=O stretching mode arising from the absorption of atmospheric CO_2 on the surface of the nanoparticles. In our study, FTIR spectroscopy of synthetic bulk ZnS after the degassing procedure showed that this sample was not oxidized, and gave a $\delta(\text{HOH})$ vibration at 1638 cm^{-1} .

¹.The 1396 cm⁻¹ bands have been assigned to the symmetric vibration of the –COO- group. Hence, we assign the 646 cm⁻¹ of Raman mode to the combinations of TO and LO modes at the H, M, and L points.

The band 1010 cm⁻¹ is strong with broadness arising from the Zn-S vibration. The 915 cm⁻¹ band is due to the C-C stretching, this carbonyl group is due to the adsorption of the residual acetate group. The Raman band at 728 cm⁻¹ is assigned to the CO₃²⁻ v₂ in-plane bending mode. According to Cheng¹² in the low-frequency region, a peak at 224 cm⁻¹ is assigned to LA overtones along M-K points, where phonon dispersion is nearly flat and hence the combination of the phonon band structure. The phonon density of states DOS is very high. Above 380 cm⁻¹, we find the acoustic and optical combinations. For instance, the broad weak peak at 414 cm⁻¹ can be assigned to TA +LO at L and M points for flat phonon dispersion in the two points. Finally, 2TA_X is measured at 179 cm⁻¹.

3. Conclusions

In conclusion, ZnS nanoparticles were synthesized through the chemical aggregation technique. The sizes of the ZnS nanoparticles were measured using the HRTEM which were between 25 and 29 nm. The HRTEM analysis showed the formation of spherical nanoparticles with hexagonal structure that coincides with database files PDF# 83-2377. The bandgap energy of ZnS nanoparticles was of 3.84 eV, which is higher than bulk ZnS (3.7 eV) showing quantum confinement.

Since ZnS nanoparticles are suspended in the residual compounds of the precursors used, the realized Raman and FTIR spectra shows a number of significant signals in the range of 1500-4000 cm⁻¹.

Acknowledgements

We thank the transmission electron microscopy laboratory of the Universidad de Sonora and the Instituto Tecnológico de Hermosillo for the facilities to measure HRTEM images and UV-vis Spectrum respectively.

References

- [1] R. M. Dziejczak, A. L. Gillian-Daniel, G. M. Petersen, K. J. Martínez-Hernández, *J. Chem. Educ.* **91**, 1710 (2014).
- [2] A. Chandran, N. Francis, T. Jose, K. C. George, *SB Academic Review* **XVII**(1 & 2), 17 (2010).
- [3] N. Üzar, M. Ç. Arikian, *Bull. Mater. Sci.* **34**(2) 287 (2011).
- [4] R. John, S. S. Florence, *Chalcogenide Letters* **6**(10), 535 (2009).
- [5] S. H. A. Allehyani, R. Seoudi, D.A. Said, A.R. Lashin, and A. Abouelsayed, *Journal of Electronic Materials*, **44**, 11 (2015).
- [6] T. T. Q. Hoa, L. V. Vu, T. D. Canh, N. N. Long, *Journal of Physics: Conference Series* **187**, 012081 (2009).
- [7] V. L. Gayou, B. Salazar-Hernández, R. D. Macuil, G. Zavala, *Journal of Nano Research*, **9**, 125 (2010).
- [8] A. K. Shahi, B. K. Pandey, R. K. Swarnkar, R. Gopal, *Applied Surface Science* **257**, 9846 (2011).
- [9] F.B. Gilbert, B. Huang, F. Lin, Z. Goodell, C. Zhang, H. Banfield, *Nano Letters* **6**, 605 (2006).
- [10] G. Murugadoss, *Journal of Luminescence* **131**(10), 2216 (2011).
- [11] A. Ghatak, G. H. Debnath, M. Mandal, P. Mukherjee, *RSC Adv.* **5**, 32920 (2015).
- [12] Y. C. Cheng, C. Q. Jin, F. Gao, X. L. Wu, W. Zhong, S. H. Li, P. K. Chu, *Journal of Applied Physics*, **106**(12), 123505 (2009).

- [13] A. S. Kumari, K. G. Mangatayaru, G. Veerabhadram, *Journal of Applied Physics* **6**(1), 1 (2013).
- [14] A. Thottoli, A. Achuthanunni, *Journal of Nanostructure in Chemistry* **3**, 31 (2013).
- [15] R. L. Frost, *Journal of Raman Spectroscopy* **42**, 1690 (2011).